1-31-2020

Characterization of friction based on specific film thickness and wettability

Avdhesh Bansal
ab1808@rit.edu

RIT

Characterization of friction based on specific film thickness and wettability

By

Avdhesh Bansal

A Thesis Submitted in Partial Fulfillment of the Requirements for the Degree of Master of Science in Mechanical Engineering

Department of Mechanical Engineering

Kate Gleason College of Engineering

Rochester Institute of Technology

Rochester, NY

January 31st, 2020

Committee Approval:

Dr. Alan Nye **Date**

Associate Department Head

Department Representative

Dr. Michael J. Schertzer **Date**

Associate Professor

Thesis Advisor

Committee Member

Dr. Patricia Iglesias Victoria **Date**

Associate Professor

Committee Member

Dr. Rui Liu **Date**

Assistant Professor

Committee Member

Abstract

Friction and wear in tribological systems lead to monetary loss and environmental damage. A better understanding of factors that affect tribological behavior of a system will reduce losses and damages in a tribological system. Wetting and surface properties are important in solid-fluid interactions and hence should be considered in lubricant-surface tribological systems. Their effects on tribological behavior are not properly understood. This study analyzed the effect of wettability on tribological systems and checked whether inclusion of wettability in the analysis of friction can lead to a more unified approach.

Wettability informs how a liquid will behave on a solid surface. Liquids with high wettability spread over the surface, and those with low wettability do not. Wettability depends on properties of not only the liquid but also the surface. The significance of wetting in tribological systems varies from system to system.

The relative importance of wetting in tribology varies with the lubrication regime under which a system operates. The lubrication regime is characterized by lambda (λ) parameter. Based on the value of λ there are three lubrication regimes: boundary, mixed, and hydrodynamic. Researchers claim that wetting and surface properties are important in boundary lubrication regime and insignificant in mixed and hydrodynamic lubrication. This research analyzed the effects of wetting in all the regimes to test this claim.

There is disagreement among scholars on how to characterize wettability in tribological systems. Some claim that a formulation of spreading parameter that comprises polar and disperse components of surface energy and surface tension provides relevant insight. Others claim that the contact angle formed between liquid and surface is a better measure of wettability. Another group of scholars claim that a non-dimensionalized spreading parameter should be used to characterize wetting. This parameter can be calculated by contact angle.

In this study, the non-dimensionalized parameter was used as it is easy to calculate. It considers non-linear relation between contact angle and wetting behavior. The results based on this parameter converge with those based on polar and disperse components to surface tension and energy. This parameter was used along with λ to check whether different friction-coefficient versus λ curves for various lubricant surface systems can collapse into one friction coefficient versus $\lambda^*|S^*|$ curve.

If various Stribeck curves for different systems can collapse into one curve, then the process of predicting friction and wear behavior would simplify, and thus the research in the field of tribology would accelerate.

TABLE OF CONTENTS

LIST OF FIGURES

LIST OF TABLES

NONMENCLATURE

Symbol	Meaning
θ	Contact angle in degrees
γ_s	Total surface energy (mJ/m^2)
$\gamma_S^D = \gamma_S^{LW}$	Dispersive component of surface energy
γ_S^P	Dispersive component of surface energy
γ_L	Total surface tension (mN/m)
$\gamma_L^D = \gamma_L^{LW}$	Dispersive component of surface tension
γ_L^P	Polar component of surface tension
γ_{SL}	Liquid-surface interfacial tension
W_A	Work of adhesion (solid liquid interface)
W_C	Work of cohesion (liquid)
S	Spreading parameter based on total surface energy and surface tension
SP	Spreading parameter derived by Kalin et al based on polar and dispersive components of surface energy and surface tension.
S^*	Non-dimensionalized spreading parameter obtained by scaling S against γ_L
SP^*	Non-dimensionalized spreading parameter obtained by scaling SP against γ_L
S**	Non-dimensionalized spreading parameter obtained by scaling S against γ_s
SP**	Non-dimensionalized spreading parameter obtained by scaling SP against γ_s
$\|S^*\|$	Absolute value of S^*
λ	Lambda Parameter
h	Fluid film thickness
h_m	Minimum fluid film thickness
h_c	Central film thickness
σ_a & σ_b	Roughness of the two surfaces on contact

U	Entrainment speed
W	Applied load
η	Fluid viscosity
R_{x1} & R_{x2}	Radii in the entrainment direction of the two contacting bodies
E_1 & E_2	Young's modulli of two contacting bodies
υ_1 & υ_2	Poisson's ratios of two contacting bodies
R'	Reduced radius in entrainment direction
E'	Reduced elastic modulus
R_x	Radius on the ball
BL	Boundary lubrication regime
ML	Mixed lubrication regime
HL	Hydrodynamic lubrication regime
IL	Ionic Liquid
ML	Magnetorheological Liquid
DLC	Diamond like carbon
PAO	Poly-alpha-olefin
DET	2-hydroxydimethylammonium 2-ethylhexanoate
EET	2-hydroxyethylammonium 2-ethylhexanoate
MET	2-hydroxymethylammonium 2-ethylhexanoate
$PDMS$	Polydimethylsiloxane

1.0 PROBLEM INTRODUCTION

Friction and wear cause monetary losses and environmental damage and reduce performance and life of machines. A comprehensive understanding of factors that affect the tribological performance of a system is necessary to reduce friction and wear [1]. Tribology is the study of friction and wear in interacting surfaces in relative motion. Hardness, surface roughness, elastic and plastic properties are important in tribological systems and have been extensively studied. Wetting and surface properties are important in solid-liquid interactions, but their effect on tribological behavior of system is not properly understood [2–6]. A comprehensive understanding of wetting and surface properties and their effect on tribological performance will boost research into new materials, lubricants, and lubrication practices. This study might help find methods to decrease the adverse effects of friction and wear.

The specific film thickness (λ) or the lambda parameter defines the lubrication regime under which a tribological system operates. It is the ratio of theoretical fluid film thickness to root mean square value of the roughness of surfaces in contact. It informs about the intensity of asperity interaction between the surfaces in a tribological system and the governing lubrication mechanism [2,6,7]. There are three lubrication regimes based on value of λ: boundary lubrication (BL) regime $(\lambda < 1)$, mixed lubrication (ML) regime$(1 < \lambda < 3)$, and hydrodynamic lubrication (HL) $(\lambda > 3)$ regime. When $\lambda < 1$, the system operates in BL regime. In BL, friction is highest because asperities of both the surfaces are in contact (Fig.1). For $1 < \lambda < 3$, the system operates in ML regime and a thin film of fluid exists between the surfaces. There is some contact between asperities and the contact pressure is shared in part by the fluid, resulting in moderate friction values. In HL, $\lambda > 3$ and a thick fluid film separates the surfaces. Friction is lowest in this regime but increases with increase in fluid film thickness [2,6,8].

Lambda compares film thickness to surface roughness of the surfaces in contact. It can be calculated using minimum film thickness (h_m) or central film thickness (h_c). The results based on both h_m and h_c are qualitatively similar, but quantitatively different. In this study, λ was calculated using h_m.

The significance of wetting in a tribological system varies with the lubrication regime under which a system operates. Scholars disagree on relative importance of wetting in different lubrication regimes. Bombard et al. claim that wetting is important in BL, but of little significance in ML and HL. In ML and HL viscosity plays a significant role [2]. Kalin et al. claim that wetting and surface energy relate with friction values in electrohydrodynamic (EHL). The interactions in EHL are governed by wetting and surface properties because only surface and lubricant interactions take place in EHL regime. The asperities on both the surfaces do not interact [4].

Wetting is a measure of how a liquid spreads over a surface. If a lubricant has high wettability, then it will spread over the surface. If it has low wettability it will not spread. It depends on properties of lubricants and surfaces in tribological systems [2–6]. Scholars disagree on how to characterize wettability in tribological applications. Kalin et al claim that a derived spreading parameter (SP) and not contact angle (θ) should be used to characterize wettability. The results based on SP converge well with wetting behavior and friction performance, and the results based on θ do not. SP considers polar and dispersive components of surface energy and surface tension. It is derived from Young's equation and

OWRK model. They found that total surface energy and dispersive component of surface energy were similar for all surfaces, but the polar surface energy varied for all surfaces. Based on this result they concluded that polar component of surface energy has a significant role in wettability [3–8]. Bombard et al. claim that contact angle (θ) should be used to characterize wettability. Their study shows that results based on θ correlate well with wettability and friction behavior. The results based on SP did not converge well with wettability and tribological behavior [2,9,10]. As per Schertzer and Iglesias a non-dimensionalized spreading parameter S^* based on contact angle should be used to characterize wettability. The results based on S^* converged well with wetting and tribological behavior [6].

The approaches to characterize wettability offered by Kalin et al. and Bombard et al. have shortcomings. SP used by Kalin et al. to characterize wettability requires a lot of rigorous calculations and experimentation [2–6]. Contact angle (θ) used by Bombard et al. is easy to calculate but should not be used alone to describe wettability. Contact angle (θ) has a nonlinear relation with wetting. Wetting relates with cosine of contact angle [2,6]. S^* proposed by Schertzer and Iglesias seems to be the best option. It can be calculated easily by measuring θ and it considers the nonlinear relation between θ and wetting behavior. The results based on S^* have a linear relation with spreading parameter (SP^*) based on polar and disperse components of surface energy and surface tension. Rigorous calculations of polar and disperse components of surface tension and surface energy provide no additional benefit [6]. Non-dimensionalized spreading parameter S^* was used to characterize wettability in this study.

Scherter and Iglesias proposed that different Stribeck curves for different surface lubricant pairs might collapse into a single friction coefficient versus $\lambda. |S^*|$ curve. If this is true, tribological behavior of a wide range of surface lubricant pairs can be predicted by measuring wettability and other parameters that are generally measured.

This thesis examined whether wettability and specific film thickness can be used to collapse different Stribeck curves of different surface lubricant systems. Schertzer and Iglesias did some preliminary analysis, but the data points were not enough to lead to a conclusion. Several experiments were conducted to collect more data points and check whether the different Stribeck curves could be collapsed into one single curve. This study also used data collected by Hong Guo on some steel specimens. This study was performed study by:

- Calculating λ, θ, and friction coefficient
    - λ values will be calculated using h_m
- Calculating S* using θ
- Plotting friction coefficient versus $\lambda. |S^*|$

2.0 THE RESEARCH QUESTION

Primary Research Question:	Can inclusion of wetting lead to a better understanding of friction behavior across a wide range of tribological systems?

The primary contribution of this work will be to check whether inclusion of wettability can collapse different Stribeck curves for different surface lubricant pairs into one friction coefficient versus $\lambda|S^*|$ curve. If desired results are achieved, then it would simplify the research in the field of friction and save time and money.

S^* seems to be a promising parameter to characterize wettability as it can be calculated by just the contact angle. It considers the non-linear relation between wetting and θ. The results based on S^* converge well with the results based on spreading parameters based on polar and dispersive components of surface energy and surface tension. This implies that there is no additional benefit in calculating polar components of surface energy and surface tension [2–7,11].

This study analyzed whether different Stribeck curves for different tribological pairs collapse into one friction co-efficient versus $\lambda. |S^*|$ curve.

3.0 LITERATURE REVIEW

Friction and wear are crucial to modern machinery that uses rolling and sliding surfaces. In US, improper attention on of effects of friction and wear amounts to a loss of 4% of gross national product. As per an estimate, approximately one-third of the global energy reserves are expended directly or indirectly on friction. If better tribological practices are employed, then an industrial nation can save an approximate 1% of its gross national product [12]. A proper understanding of effects of all the factors that influence tribological performance is crucial to reduce friction and wear [13]. Expected savings from research in the field of tribology is estimated to be 50 times the research cost [12]. The effect of wetting and surface properties on tribological behavior of a system has not been fully understood [5,7,11]. A comprehensive understanding of effects of these factors will propel the research in the field of tribology. Such a research might lead to methods and materials to reduce friction and wear.

The specific film thickness (λ) is used to identify the lubrication regime under which a tribological system operates. It provides a measure of intensity of asperity interactions in lubricated sliding [6,8,11,12]. It is defined as the ratio of theoretical film thickness (h) to root mean square of roughness of the surfaces in contact and is described as [6,11,12,14]:

$$\lambda = \frac{h}{\sqrt{\sigma_a^2 + \sigma_b^2}} \tag{1}$$

where σ_a and σ_b are the roughness values of surfaces in contact.

Based on values of λ, tribological systems can be characterized in three regimes (Fig. 1) [6,8,11,12]:

- Boundary lubrication (BL): $\boldsymbol{\lambda < 1}$
    - The asperities on both the surfaces are in contact with each other and the load is supported by these asperities.
    - The friction values are highest in this regime.
- Mixed Lubrication:$\boldsymbol{1 < \lambda < 3}$
    - Some contact exists between the asperities and a thin fluid film separates the surfaces.
    - The load is supported by asperities and the fluid film.
    - The friction values are moderate in this regime.
- Hydrodynamic Lubrication:$\boldsymbol{\lambda > 3}$
    - The asperities on both the surface do not touch each other and a thick film of fluid separates the two surfaces.
    - The load is supported by the fluid film and the friction values are lowest in this regime.

- The friction values in this regime increase with viscous effects.

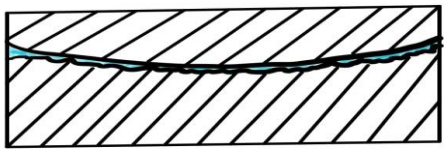

Boundary lubrication

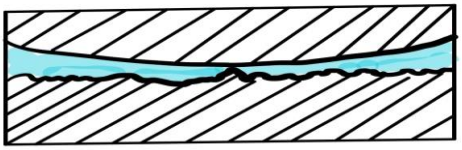

Mixed lubrication

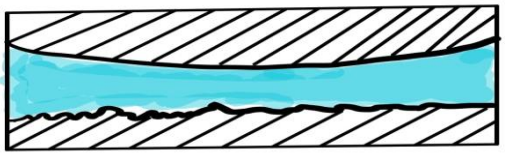

Hydrodynamic lubrication

Figure 1: Different lubrication regimes under which a tribological system operates [12]

Different definitions exist for λ depending on the type of theoretical film thickness employed for calculation [8,11,14–18]. Theoretical film thickness is calculated with the assumption that system operates in HL regime. This study employs a soft surface (PDMS) and a hard surface (steel) for the study. The surface roughness of the soft surface changes when a soft surface is used against a hard surface for tribological tests at high pressure. This change in surface roughness alters the value of λ [19]. In this study, it was assumed that the surface roughness of the soft surface remained constant. The change in surface roughness and λ were left for consideration in future studies. Theoretical film thickness in eq(1) can be calculated either by central film thickness (h_c) or minimum film thickness (h_m). Central film thickness (h_c) is the thickness of the lubricant film at the center of contact when the system and minimum film thickness (h_m) is the thickness of the fluid film at the rear or sides of contact [20]. λ values calculated using h_c are higher (not more than 2 orders) than the values calculated using h_m [11]. But the λ values obtained using h_c and h_m lead to similar tribological results. In this study, different values of λ were calculated based on minimum film thickness (h_m) (Eq.(3)) [8,11,14–18,21–24]. There is lot of data on λ based on h_m that could be used as reference for calculations in this study.

$$h_c \approx 3.3R_x^{0.80}(U\eta)^{0.64}W^{-0.22}E'^{-0.42} \quad (2)$$

$$h_m \approx 2.8R_x^{0.77}(U\eta)^{0.65}W^{-0.21}E'^{-0.44} \quad (3)$$

Where U is the entrainment speed, W is applied load, E' is reduced elastic modulus, E_1 & E_2 are elastic modulus of the surfaces in contact, and η_0, η_{40} & η_{100} are dynamic viscosities of the lubricant at operating temperature, 40°C, and 100°C respectively.

The importance of wetting in a tribological system varies with the lubrication regime in which a system operates. Scholars disagree on the regimes in which wetting plays and important role. Bombard et al. claim that wetting plays a crucial role in BL and has negligible role in ML and HL. They claim that in ML and HL viscosity plays an important role and wetting does not play a significant role as a large fluid film separates the surfaces[9]. Kalin et al. claim that that wetting plays a significant role in elasto-hydrodynamic (EHL) regime and does relate well with the friction results in BL and ML regimes. The solid surfaces do not interact in HL regime and barely in ML regime as a complete lubrication film is formed. Solid-liquid interactions become pronounced and hence wetting or surface properties play a significant role in EHL and ML [4].

Bombard et al. claim that wetting plays a crucial role in BL but not in ML and HL. Bombard et al. conducted their study on three surface pairs: Steel-Steel, POM-POM, and PDMS-PDMS. They used PAO, ionic liquids (ILs), and IL based magnetorheological (MR) fluids. All the surface lubricant pairs for steel-steel and POM-POM surfaces operate in BL ($\lambda < 1$), whereas all the PDMS-PDMS surfaces operate in ML and HL ($2 < \lambda < 22$). They found that friction does not relate well with viscosity of fluids in BL regime. They plotted a friction coefficient versus viscosity curve to analyze the effect of viscosity on friction. They found that even though viscosity values of $[BMIM^+][PF_6^-]$ and $[BMIM^+][CH_3COO^-]$ are similar, the friction coefficient of $[BMIM^+][CH_3COO^-]$ on steel-steel surface is higher than friction coefficient of $[BMIM^+][PF_6^-]$ on same surface. They also found that friction coefficient values for $[BMIM^+][PF_6^-]$ and $CYPHOS^{®}IL\ 104$ are similar, but the viscosity of $CYPHOS^{®}IL\ 104$ is higher than that of $[BMIM^+][PF_6^-]$. They then compared the friction value results at same λ value and found that the contribution of viscosity to friction minimized and friction seemed to depend on other surface properties. They concluded that viscosity does not play a significant role in BL. There were still some outliers in the results based on λ, so they analyzed the friction results based on wetting. They found that friction results aligned well with the wetting behavior. In PDMS-PDMS surfaces friction values remained almost equal for all lubricants at the same λ value. They concluded that in HL regime viscosity dominates the tribological behavior. They also concluded that wetting does not play a significant role in HL, as the friction coefficient values for all the lubricants were similar even when all lubricants had different wetting behavior [11].

Kalin et al. claim that wettability and surface properties correlate well with friction behavior in elasto-hydrodynamic (EHL) regime. Wettability does not relate well with friction behavior in BL and ML regimes [4]. They used five DLC coatings: 2 doped and 3 non-doped, and two lubricants: PAO4 and PAO9. The surfaces in EHL are separated by a thick fluid film, and there is no contact between the surfaces in a tribological system. The tribological performance in EHL varies with solid liquid

interactions. These interactions are characterized by wetting and surface properties. The asperities in BL and ML are in contact with each other, and the tribological behavior is influenced by solid-solid interactions. Wetting and surface properties do not play a significant role in these interactions [3,4,7,8].

Wettability is a measure of how liquid spreads over a surface. A liquid with high wettability spreads over the surface and a lubricant with low wettability does not spread and retains its shape. Wettability depends on the properties of lubricants and surfaces in a tribological system [5,6,11,14]. Wettability is often characterized using contact angle (θ) or spreading parameter. Contact angle is the angle that lubricant interface makes with the surface at the three-phase contact line. Liquids with low wettability form high contact angle with the surface and liquids with high wettability form small contact angle with the surface. Spreading parameter (S) (Eq.11) measures the difference between surface energy of a dry surface (γ_{SM}) and surface energy of a fully wetted surface ($\gamma_{SL} + \gamma_{LM}$). It is a measure of difference between work of adhesion (W_A) between surface and lubricant, and work of cohesion (W_C) between lubricant molecules. There is a disagreement on how to characterize wettability.

$$S = W_A - W_C = \gamma_{SM} - (\gamma_{SL} + \gamma_{LM}) \tag{4}$$

Researchers in tribology disagree on what parameter to use to characterize wettability. Kalin et al. believe wetting should be characterized using a derived spreading parameter (SP) (Eq.12). They compared wetting results based on θ and SP with actual performance. They found that θ formed by lubricants on DLC surfaces (except F-DLC) is lower than θ formed by lubricants on steel. This implies that DLCs have better wettability than steel. The results are contradictory to the behavior of DLCs, as they have a poor wetting behavior when compared to steel. Also, the results vary with the lubricant used. The value of θ formed by N-DLC with PAO4 is lower than θ formed by steel with the same lubricant, but N-DLC forms higher θ with PAO9 than steel does with PAO9. The results based on θ are not consistent for the two lubricants. But the results of SP align with wetting behavior of DLCs. The results based on SP demonstrated that DLCs (except ta:C) have lower wettability with steel. The results are consistent for both the lubricants.

SP (Eq.11) is derived from S (Eq.9) using Young's equation [25] (Eq.5) and OWRK model (Eq.6) [26]. SP considers polar (γ_S^P) and dispersive (γ_S^D) components of surface energy of the surface, and polar (γ_L^P) and dispersive (γ_L^D) components of surface tension of the lubricant. They found that the total surface energy and dispersive energy of the surface are similar, but the polar component of surface energy varies significantly from surface to surface. They concluded that the difference in total surface energy is due to polar component of surface energy. They also claimed that polar component of surface energy plays the most important role in wetting behavior of a tribological system

$$\gamma_{SM} - \gamma_{SL} = \gamma_{LM} \cos\theta \tag{5}$$

$$\gamma_L(1 + cos\theta) = 2\left(\sqrt{\gamma_S^D \gamma_L^D} + \sqrt{\gamma_S^P \gamma_L^P}\right) \tag{6}$$

Substituting (5) into (4)

$$S = \gamma_{LM}\cos\theta - \gamma_{LM} = \gamma_{LM}(cos\theta - 1) \quad (7)$$

Equation (7) can also be described as

$$S \approx \gamma_{LM}(\cos\theta + 1) - 2\gamma_{LM} \quad (8)$$

Substituting OWRK model (6) in (8) yields spreading parameter (SP) proposed by Kalin et al.

$$SP = 2\left(\sqrt{\gamma_S^D\gamma_L^D} + \sqrt{\gamma_S^P\gamma_L^P} - \gamma_{LM}\right) \quad (9)$$

Bombard et al. claim that contact angle (θ) should be used to characterize wettability. They used SP used by Kalin et al. and θ to characterize wettability. They compared the results based on SP and θ with wetting and friction behavior. They found that results based on θ converge better with wetting behavior and friction performance than results based on SP (Fig 3, 4a), 4b)). They found that friction values in BL regime (steel-steel and POM-POM) correlated well with contact angle and not with SP. It is easy to characterize wetting using θ and does not require a lot of rigorous calculations [11]. But, θ alone should not be used to characterize wetting because θ has a nonlinear relation with wetting. Wettability relates with cosine of θ [5,6,14].

Schertzer et al. proposed that a non-dimensionalized spreading parameter (S^*) based on θ should be used to characterize wettability. They compared wettability results based on θ, S, SP, and some non-dimensionalized spreading parameters. These non-dimensionalized spreading parameters were obtained by scaling S and SP against surface tension and surface energy. They demonstrated that S can be expressed as a function of θ using Young's equation [27](Eq.7). Using Eq.7 and Eq.10 they incorporated θ in S and expressed it as difference between work of adhesion and work of cohesion [6,27]:

Work of adhesion is described as

$$W_A \approx \gamma_{LM}(\cos\theta + 1) \quad (10)$$

Using Eq.10 in Eq. 8

$$S \approx W_A - W_C \approx \gamma_{LM}(cos\theta + 1) - 2\gamma_{LM} \quad (11)$$

They first compared the wettability results of S, θ, and SP. They found that S and SP correlate with θ. S has a better correlation with θ, as S can be expressed as an explicit function of contact angle. The relation between S, SP and θ is nonlinear, suggesting θ alone should not be used to characterize wettability. But, the relation between S and SP is linear. This means that wettability results based on S and SP are similar [6]. They then compared different non-dimensionalized spreading parameters. These parameters are constructed by scaling S and SP against surface energy of the surface (γ_S) or surface tension between the liquid and the surrounding medium (γ_{LM}). Based on Eq.9 and Eq. 11, these non-dimensionalized spreading parameters are as follows [6]:

$$S^* = S/\gamma_{LM} = (cos\theta - 1) \tag{12}$$

$$SP^* = SP/\gamma_{LM} = 2\left(\sqrt{\frac{\gamma_S^D \gamma_L^D}{\gamma_{LM}^2}} + \sqrt{\frac{\gamma_S^P \gamma_L^P}{\gamma_{LM}^2}} - 1\right) \tag{13}$$

$$S^{**} = S/\gamma_S = (\gamma_{LM}/\gamma_S)(cos\theta - 1) \tag{14}$$

$$SP^{**} = SP/\gamma_S = 2\left(\sqrt{\frac{\gamma_S^D \gamma_L^D}{\gamma_S^2}} + \sqrt{\frac{\gamma_S^P \gamma_L^P}{\gamma_S^2}} - \frac{\gamma_{LM}}{\gamma_S}\right) \tag{15}$$

They found that all the non-dimensionalized spreading parameters from Eq.12 to Eq.13 have a nonlinear relation with θ [6]. They also found that non-dimensionalized parameters based on contact angle have a linear relation with those based on polar and dispersive components of surface tension and surface energy. S^* related linearly with SP^* and S^{**} related linearly with SP^{**}. This implies that calculation of polar and disperse components of surface would not provide any additional benefit, as the parameters based on contact angle correlate with parameters based on polar and disperse components of surface tension and surface energy. So, they concluded that parameters based on contact angle should be used to characterize wetting as they require fewer inputs. Hence, they proposed that S^* (Eq.16) should be used to characterize wetting as it can be calculated by measuring contact angle.

The approaches offered by Kalin et al.(SP) and Bombard et al. (θ) have shortcomings. Measurement of SP involves rigorous calculation (Eq.12), as polar and dispersive components of surface tension and surface energy must be calculated to calculate SP. [3–7,11]. It is easy to characterize wetting using θ and does not require a lot of rigorous calculations [11]. But, θ alone should not be used to characterize wetting because θ has a nonlinear relation with wetting. Wettability relates with cosine of θ [5,6,14]. The use of contact angle alone to characterize wetting can lead to inaccuracy. This is because depending on the relative strength of work of adhesion and work of cohesion the time required for a liquid to form a stable contact angle may vary [3–7]. S^* proposed by Schertzer et al. provides a solution to these shortcomings. It is easy to calculate, as it only needs θ as input, and it takes into consideration the nonlinear relation between θ and wettability (Eq.16). S^* also has a linear relation with non-dimensionalized spreading parameter based on polar and dispersive components of surface tension and surface energy. This means that there is no additional benefit in calculating polar and disperse components of surface tension and surface energy. This study employed S^* to characterize wettability.

Schertzer et al. also characterized friction using S^*. They started by plotting friction coefficient against λ. Friction coefficients are low when $\lambda > 1$. For $\lambda < 1$, friction coefficients are high when $|S^*| < 0.1$ and moderate when $0.1 < |S^*| < 1$. There are several outliers in this plot. IL104 records moderate friction values on steel-steel surface even when value of $|S^*|$ is low, and PAO and IL104 records low friction values on PDMS-PDMS surface when $|S^*|$ is moderate. They then plotted λ versus $|S^*|$ plot to analyze the relation between λ and $|S^*|$. They found that when speed is varied at constant load, $|S^*|$ does not change and the values on the plot fall into vertical groups. λ increases with speed for a given value of

$|S^*|$. These observations imply that λ and $|S^*|$ are independent variables. They then plotted friction coefficient versus $\lambda|S^*|$ plot and based on the plot identified three regimes [6]:

- When $\lambda|S^*| > 0.5$
    - Friction coefficients are generally low and consistent
    - Corresponds to HL regime
- When $10^{-3} < \lambda|S^*| < 0.5$
    - Friction coefficients increases moderately
    - Corresponds to ML regime
    - Moderate values of λ reduce friction values when $|S^*|$ is small
    - Moderate values of $|S^*|$ reduce friction values when λ is small
- When $\lambda|S^*| < 10^{-3}$
    - Frictions increases drastically
    - Values of both λ and $|S^*|$ are small

Based on the results, Schertzer et al. proposed that friction behavior of tribological systems can be predicted by calculating λ and $|S^*|$. They also suggested that different Stribeck curves for different surface lubricant pairs might collapse if a non-dimensionalized spreading parameter is also considered along with λ.

This study checked whether different Stribeck curves for different lubricants could be collapsed into one friction coefficient versus $\lambda|S^*|$. Schertzer et al. had done some preliminary meta-analysis with data from [5,11,28]. In this study, experiments and calculations were performed with PDMS surface and AISI52100 steel balls and four lubricants: PAO40, and three ILs. Enough data points were collected to analyze and check whether different Stribeck curves can collapse.

4.0 OBJECTIVES OF THE PROPOSED WORK

The main purpose of this work was to test whether the different Stribeck curves obtained for different surface lubricant combinations can collapse into one friction versus $\lambda.|S^*|$ curve (Fig.12). To achieve this, the value of λ for different combinations of applied load and speed on different surface lubricant pairs was calculated, and several experiments to measure contact angle and friction coefficient were conducted. This study employed PDMS surface and four lubricants: PAO40, and 3 ILs (DET, EET, and MET). Also data on steel-steel surface and DET, EET, and MET was taken from a study conducted by Hong Guo.

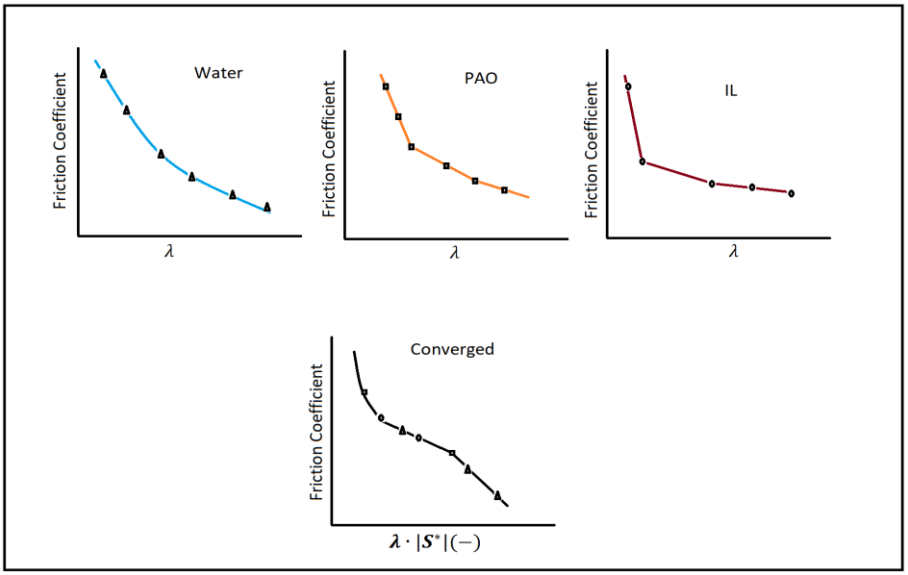

Figure 2: The primary goal is to collapse different curves for friction coefficient for different systems into one curve using S*. (This graph is a hypothetical sketch and is not based on real values.)

As per eq (1), λ is a function of fluid film thickness (h) and root mean square value of surface roughness. One can choose between two values of h: central film thickness (h_c) and minimum film thickness (h_m). Lambda was calculated with h_m. Based on equation (6), h_m depends on entrainment speed (U), fluid viscosity (η), applied load (W), radius of the ball (R_x), and reduced modulus of elasticity (E'). Out of these parameters, η has a constant value and the value is different for different fluids. The balls with the same radius (R_x) were used for all experiments. Experiments were performed at different loads (W) and different speeds (U) to obtain different values of λ. The value of S* is a function of contact angle (Eq.16).

After the experiments, the friction coefficient was plotted as a function of λ, and then as a function of $\lambda.|S^*|$ and the two plots were compared to check whether our goal is met.

In this study, PDMS 184 was used for surface, AISI 52100 for steel balls, and PAO 40, and three ionic liquids for lubricants. PDMS was chosen as because all the three lubrication regimes $(BL, ML, and\ HL)$ could be achieved on PDMS, and also because many tribological studies in [11] have been done on PDMS. There is a lot of data to refer to and compare results with. PAO 40 was employed for the study because results based on PAO would serve as reference for results based on ILs. DET, EET, and MET

were chosen as ILs because these three ILs have similar chemical composition but have different viscosities and tribological behavior. A proper analysis of their behavior helped us check the tribological behavior in the three lubrication regimes: $BL, ML, and\ HL$.

Description of methods and experiments:

- **Contact angle ($\boldsymbol{\theta}$):** The contact angle was calculated using Rame-Hart contact angle goniometers. The contact angles were measured using DROPimage software.
- **Friction coefficient:** This was measured using ball-on-flat tribometer. The friction coefficients were measured at different values of λ, by varying the applied load (W) and the entrainment speed (U). The tribometer is operated using Lab View.

5.0 EXPERIMENTAL METHODOLOGY

Derived Data

Tribological data pertaining to steel-steel surfaces tested with ionic liquids was obtained from Hong Guo. Hong performed tribological tests for AISI 52100 steel balls and surfaces with three ionic liquids: DET, EET, and MET. She used steel balls of 1.5mm diameter and of 0.5 μm surface roughness. She used steel surface of 3.125 cm diameter. The surface was polished to a surface roughness of 0.01 μm. The friction tests were conducted on a reciprocating tribometer at a constant speed of 0.03 m/s (5Hz frequency and 3 mm stroke length) and at a constant load of 3 N. Each test was run for 3600 seconds (1 hours) to cover a distance of 108 meters.

Materials and Preparation

In the study, PDMS surface, AISI 52100 steel balls, and four lubricants were used. The steel balls of diameter of 1.5 mm and surface roughness of 0.05 μm were bought from a supplier. The PDMS surfaces of diameter of 1.251 inches and a height of 1 cm were cast using a mold. One of the surfaces of the mold was polished to achieve a surface roughness of 0.5 μm. For each specimen, the elastomer base and the elastomer curing agent were mixed in a ratio of 10:1. This mixture was then deaired for 2 hours. The solution was then poured into the mold. The mold was then placed in vacuum for 6 hours to remove entrapped air bubbles. After this process, the mold was placed in a furnace for 12 hours at 65 $°C$. The prepared specimen was removed from the mold after baking. Four lubricants were used for the study: PAO 40, DET, MET, and EET (Table1). Out of the four lubricants, PAO 40 was sourced from market and the other three lubricants were synthesized by Hong Guo.

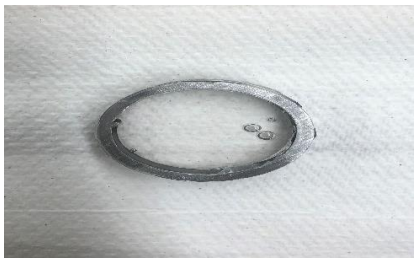

Figure 3: PDMS Specimen

Figure 4: Mold: (left to right) bottom plate, polished surface, cavity, and top plate

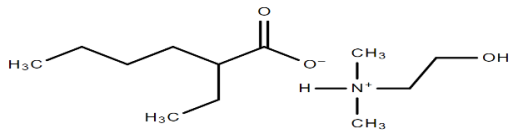

(DET)

2-hydroxydimethylammonium 2-ethylhexanoate

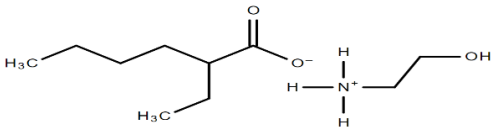

(EET)

2-hydroxyethylammonium 2-ethylhexanoate

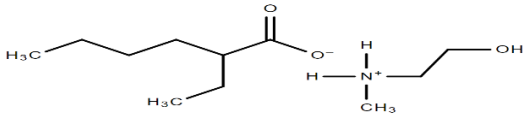

(MET)

2-hydroxymethylammonium 2-ethylhexanoate

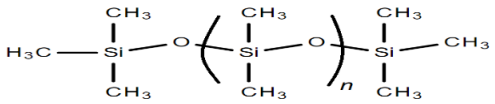

(PDMS)

Polydimethylsiloxane

Figure 5: Molecular structures of EET, MET, DET, and PDMS[29][30]**.**

Experimental Details

Surface Roughness: The steel balls of 0.05 μm surface roughness were outsourced. For the PDMS surface a surface roughness of 0.5 μm was obtained by polishing a flat surface of a cylindrical steel specimen to the desired surface roughness. This polished specimen was then fitted in the mold and polymer poured over it to achieve the desired roughness. The surface roughness of the steel specimen was measured using optical profilometer NONOVEA ST400 (Fig.13). It measures wavelengths directly related to specific heights and then calculates the average roughness values for the surface (Fig.14). The steel specimen was placed on a platform below the lens. The area to be analyzed was demarcated using a computer software. The profilometer then performed the scan and returned the average value for surface roughness. For this study, three measurements of surface roughness were taken, and the average value of these readings was used.

Figure 6: NONOVEA ST400

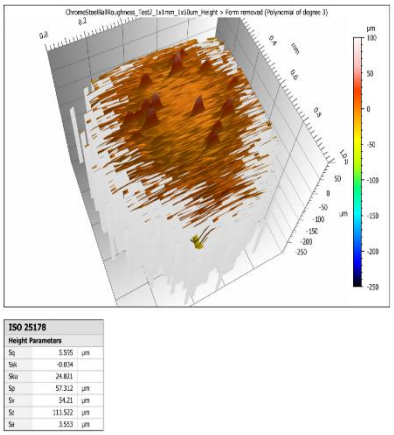

Figure 7: Surface roughness calculation of AISI 52100 1.5 mm diameter steel ball using NONOVEA ST400.

Material	Roughness
PDMS	0.5μm
AISI 52100	0.05μm

Table 1 Surface roughness values for PDMS and AISI 52100.

Friction Coefficient: Friction coefficients were measured using ball-on-flat or reciprocating tribometer. In a ball-on-flat tribometer one can conduct multiple tests on the same surface, but its sliding speed is limited. The speed varies in a ball-on-flat tribometer as the steel ball slides over the surface from one end to other, but the sliding speed is assumed to be constant. The various parts of a tribometer and steps involved in measurement are shown in Fig.8. The tribometer is set in such a way that the applied load acts normal to the surface. The applied load can be modulated by changing the weights on the

device. The sliding speed and sliding time are set up using Lab View. The strain gauge is attached to the arm of the arm of tribometer. As the pin runs on the sample the strain generated in measured by the strain gauge. This strain value is used to calculate friction, and then friction coefficient using lab view. Strain and friction are related as per the eq. 16. Where L is length of the arm, w is width of the arm, E is elastic modulus of the arm, h is the height of the arm, and F is friction [27].

$$\epsilon = \frac{6FL}{wh^2E} \tag{16}$$

A drop of lubricant is placed between the surfaces in contact and the sliding speed is set on Lab View software, and the applied load is manually placed on the tribometer. The tribological behavior of different surface lubricant pairs was studied under different lubrication regimes. The entrainment speed (U) and applied load (W) were varied to operate the system in different lubrication regimes (different λ values). The friction coefficient was recorded for a sliding distance of 100 meters at different speeds. The time for each experiment varied from 33 minutes 20 seconds to 2 hours 46 minutes 40 seconds, depending on the entrainment speed. Before each experiment the surface was washed, the steel ball was replaced, and 3 calibration readings were taken. The calibration readings were taken keeping the pin still on the surface. For each calibration reading, the stroke length was set to zero, and the load and frequency were set to the values the system would operate in for the experiment for which the calibration was being done. Each calibration test was run for 3 minutes. Ideally, when the piston is still (zero stroke length), the average friction value should be zero. The average of each calibration was taken and then an average of average of values of three calibration tests was taken. This value was later subtracted from the average of the results of tribological experiment. At least three data points were recorded for each selected combination of speed, load, and surface lubricant pair.

The results were categorized based on value of λ. This categorization was then compared to categorization based on $\lambda|S^*|$. In this study, 4 surface-lubricant pairs were employed, and 28 tests were conducted. This study analyzed the tribological behavior of systems in different regimes and tested for λ values ranging from 0.002 to 3.86. This means that tribological behavior in all the three regimes $(BL, ML, and\ HL)$ was observed. The friction data for each case was also plotted against time (Fig.9) to check whether the system reached a steady state. All the cases in this study reach a stable state within the first 200 seconds. This study also used friction data for steel surface and steel balls with DET, EET, and MET collected by Hong Guo in her study.

a)

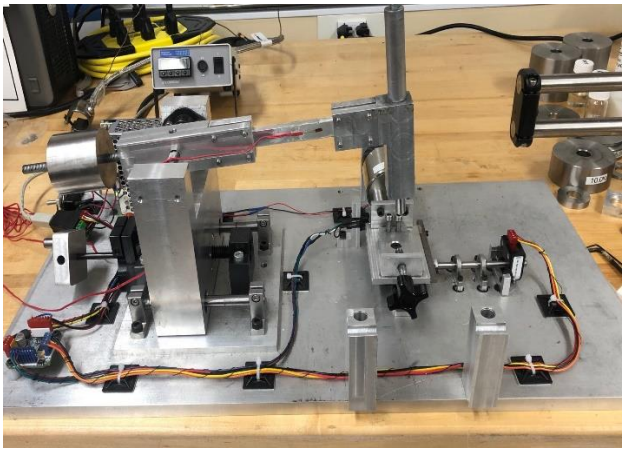

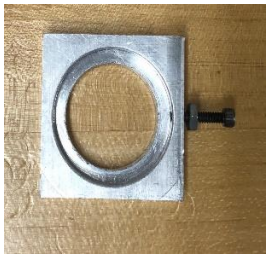

b)

c)

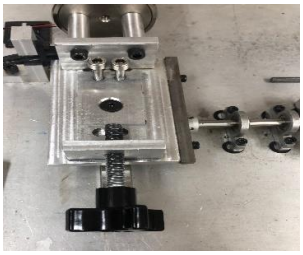

d)

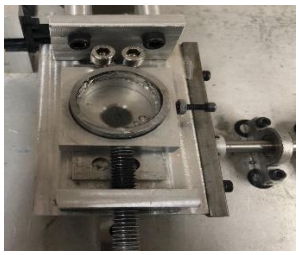

e)

f)

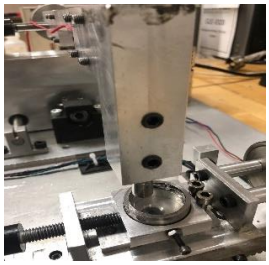

g)

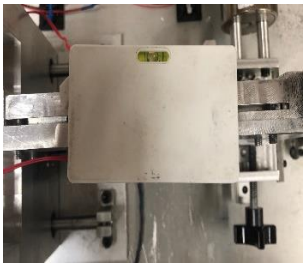

h)

Figure 8: a) Reciprocating Tribometer b) sample holder c) sample to be tested d) reciprocating platform e) sample holder attached f) ball is loaded on the pin g) pin is installed on tribometer h) the sample is levelled [31]**.**

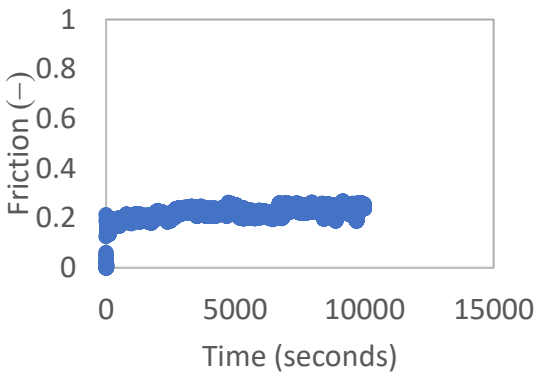

Figure 9: PAO-PDMS friction against time for BL at 3 N and 0.01 m/s . The time series for all the cases in this study were similar.

The PDMS and PAO pair was tested for a value of λ ranging from 0.86 to 3.10 (Table 2). The respective values of λ were achieved by varying load and speed. For DET and PAO, the system always operated in BL regime $(\lambda < 1)$. In this study DET and PDMS pair was tested for a λ value of 0.58. For PDMS and EET pair the system always operated in HL regime $(\lambda > 3)$. PDMS and EET pair was tested for λ value of 3.86. The PDMS and MET pair was tested for a λ value ranging from 0.946 to 3.109. In case of steel surface and steel balls, the λ was always less than one. The tribological data for steel surfaces and ionic liquids was obtained from Hong Guo. Hong Guo used AISI 52100 steel surface and balls for her study. For all the cases, she ran the system at a constant speed of 0.03m/s (stroke length of 3mm and frequency of 5Hz) and at a constant load of 3N. Each experiment was conducted for a sliding distance of 108 meters and it took about 1 hour to complete each experiment.

Surface	Lubricant	$Load$ (N)	$Speed$ $\left(\frac{m}{s}\right)$	$Time$	λ	$Regime\ as\ per$ λ	$Uncertainty$ $for\ \lambda$
PDMS	PAO40	1	0.05	33m20s	3.095	HL	±0.003
PDMS	PAO40	3	0.05	33m20s	2.458	ML	±0.0003
PDMS	PAO40	3	0.01	2h46m20s	0.863	BL	±0.001
PDMS	DET	1	0.05	33m20s	0.58	BL	±0.001
PDMS	EET	3.98	0.01	2h40m20s	3.86	HL	±0.004
PDMS	MET	1.5	0.05	33m20s	3.109	HL	±0.003
PDMS	MET	2.5	0.04	46m40s	2.416	ML	±0.003
PDMS	MET	3.98	0.01	2h46m20s	0.889	BL	±0.007
Steel	DET	3	0.03	1 hour	0.00291	BL	±0.0003
Steel	EET	3	0.03	1 hour	0.07361	BL	±0.008
Steel	MET	3	0.03	1 hour	0.01694	BL	±0.002

Table 2 Load, speed, time taken for each experiment, λ, and characterization of lubrication regime based on λ for all lubricants (PAO40, DET, EET, and MET) on different surface pairs (PDMS-steel and steel-steel). The uncertainty is calculated at 2 standard deviations at 95 % confidence interval.

Contact Angle (θ): The contact angle measurements were made before the experiments for each surface lubricant pair. Contact angle was measured using Ramé-Hart goniometer (Fig. 10). The system was calibrated prior to starting the measurements. The surface is placed on the stage and the height of the stage is adjusted to bring the surface into view. Then a drop is placed on the surface and the camera is focused on the drop. Once focus is set, then a horizontal reference axis is set right above the surface. Then either one vertical axis is set passing through the center of the drop or two vertical axes are set to remove the area with reflection of light. In this study, two vertical axes were set to remove the area with reflection from analysis. Then number of observations per second and duration for the observation are set using DROPimage advanced software (Fig. 11). The software also records standard deviation, range and mean of the contact values. Each contact angle test was conducted for 300 seconds. For every surface-lubricant pair the measurements were taken at least three times, and four times if there was a huge difference between the results of first two experiments. After each measurement the surface was cleaned.

a) 

b) 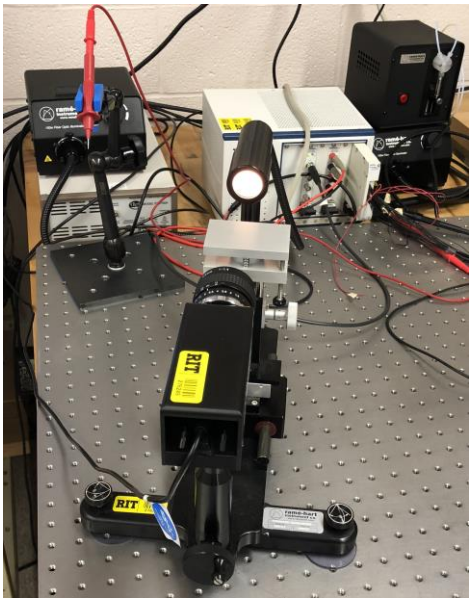

Figure 10: Ramé-Hart goniometer at Digital Microfluidics lab.

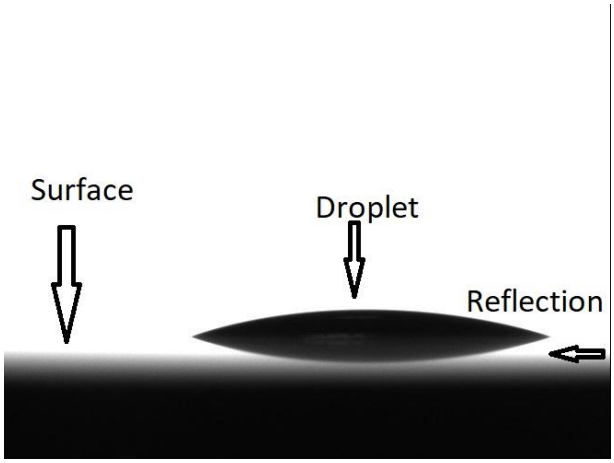

Figure 11: PAO40 droplet on AISI 316 surface. The measurements were made on Ramé-Hart goniometer.

6.0 RESULTS AND DISCUSSION

In this section, friction results are compared against different parameters: viscosity, contact angle (θ), spreading parameter (S^*), specific film thickness (λ), and a combination of specific film thickness and spreading parameter $(\lambda|S^*|)$. The outliers for characterization based on different parameters are shown and drawbacks of the characterization discussed. At the end, the characterization based on $\lambda|S^*|$ is shown and its advantages over characterization based on other parameters discussed.

6.1 Characterization based on viscosity

An attempt was made to characterize friction data based on viscosity (Fig.12). The friction in the system decreases as a more viscous lubricant is used. If the system operates in HL regime then beyond a certain point, the friction increases as viscosity increases. It was expected that the friction values would decrease with more viscous lubricants. The lambda (λ) can be increased by either increasing the operating speed or lowering the applied load. This means that as load and speed are altered the lubrication regime under which a system operates changes. This transition of regime would alter the friction results for the same surface lubricant pair. It was found that for same lubricant friction coefficient decreased with increase in speed. The friction coefficient also decreased as viscosity increased. But there were some outliers. The lowest friction values were recorded for PDMS-DET pair even when DET has the lowest viscosity. EET-PDMS pair recorded a high value of friction even when EET has the highest viscosity of all the lubricants. MET and PAO have similar viscosities but the friction values were different. For the same lubricant surface pair (PDMS with PAO and MET), different friction values were recorded depending on the operating conditions. Based on evidence, viscosity should not be used to characterize friction. Some other surface properties (lambda or wettability) should be used to characterize friction.

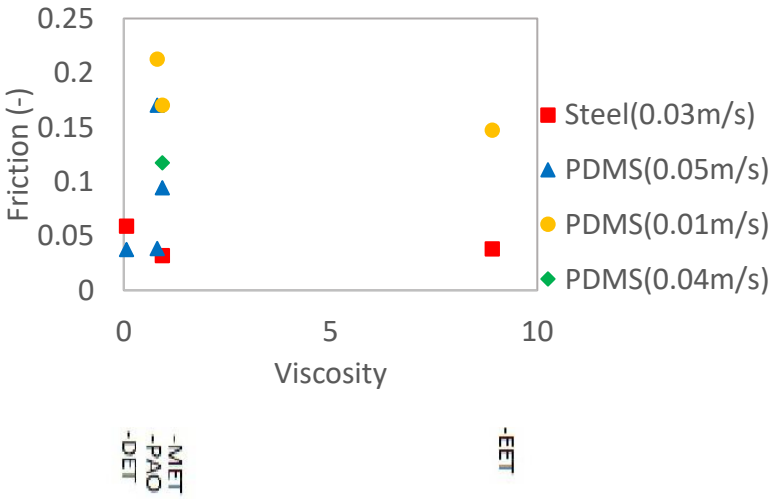

Figure 12: Friction versus viscosity for steel-steel surfaces at 0.03 m/s (red square) and PDMS-steel surfaces at 0.01 m/s (yellow dot), 0.04m/s (green), and 0.05 m/s (blue triangle) for different lubricants.

Then friction against viscosity data was compared on basis of λ value (Fig.13). The contribution of viscosity to friction was minimized. The value of friction decreased as value of λ increased. The friction decreased as system transitioned from BL to HL. There were some still outliers. The friction values for steel were low even when the λ values were low. For $\lambda < 1$, PDMS surface in one case recorded a low friction value. When $\lambda < 1$, a system should operate in BL and the friction values are high. For $\lambda > 3$, PDMS surface in one case recorded a high friction. In HL $(\lambda > 3)$, a system generally records low friction values. The classification based on λ better characterized friction than viscosity, but still there were still some outliers. So, lambda alone is not enough to characterize friction and other surface properties should be taken into consideration.

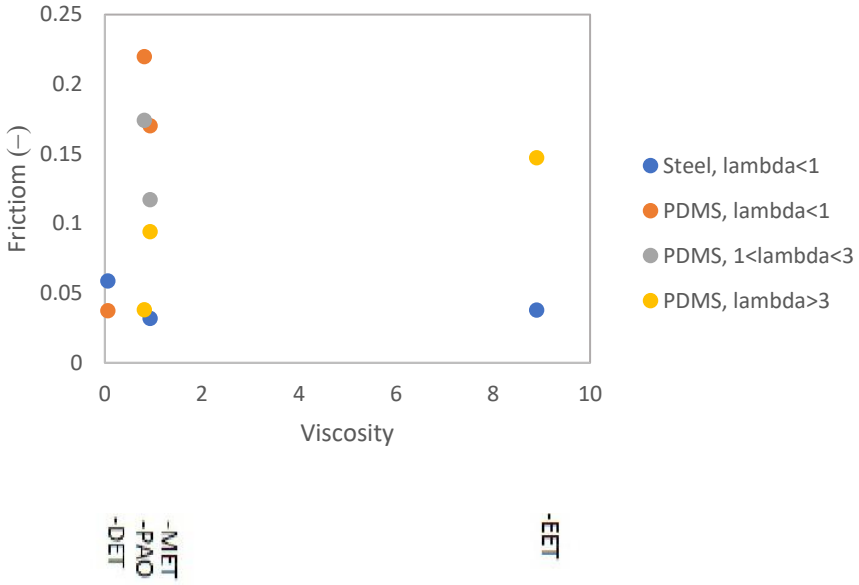

Figure 13: Friction versus viscosity for steel-steel surfaces for steel at $\lambda < 1$ (BL), for PDMS at $\lambda < 1$ (BL), $1 < \lambda < 3$ (ML), and $\lambda > 3$ (HL) for different lubricants.

6.2 Characterization based on contact angle (θ)

As per Bombard et al., wetting plays a significant role in BL. It is preferable to have high wettability for a system that operates in BL. A wetting liquid has higher wettability when the contact angle is low and vice versa[32]. The lubricant spreads over the surface and fills the asperities and reduces friction. It was expected that friction would decrease for systems operating in BL with decrease in contact angle. Low wettability is preferred for systems operating in ML and HL regime. The load is supported by the lubricant and the surfaces are either in partial contact or no contact at all. It is desired that a lubricant operating in ML or HL keeps the surfaces separated and does not spread over the surface. The friction in ML and HL increases with increase in wettability. This means that the friction values in ML and HL were expected to increase with decrease in contact angle [4,6,11].

The study found that when PDMS was used with PAO and MET in BL, lower friction value was recorded for a lower contact angle (PAO) (Fig 14, Table 3, and Fig.15). For PDMS operating in ML and HL, the study found that lubricant with higher contact angle recorded lower friction values (MET). PDMS-EET

pair operated in HL and recorded very low contact angle. The pair recorded the highest value for friction among all systems operating in HL and the value was higher than expected. PDMS-DET pair operated in BL and recorded the lowest contact angle among all system PDMS systems operating in BL regime. The pair recorded the lowest friction among all PDMS systems in BL but the friction value was lower than expected. Steel-steel surface pairs recorded contact angles lower than PDMS-steel pairs (Fig.14 and 16, and Table 4). Steel-DET recorded the lowest contact angle but recorded the highest friction among all the steel-steel systems. The friction values recorded by all steel-steel system cases were lower than the PDMS-steel cases, but the values were lower than expected.

Contact angle could not fully characterize friction because in some cases the values were very different from the expected. The possible reason for this behavior is that all the systems were operated in varied conditions and contact angle alone cannot take into account the effect of change in operating conditions. Specific fluid film thickness (λ) takes into account the change in operating conditions.

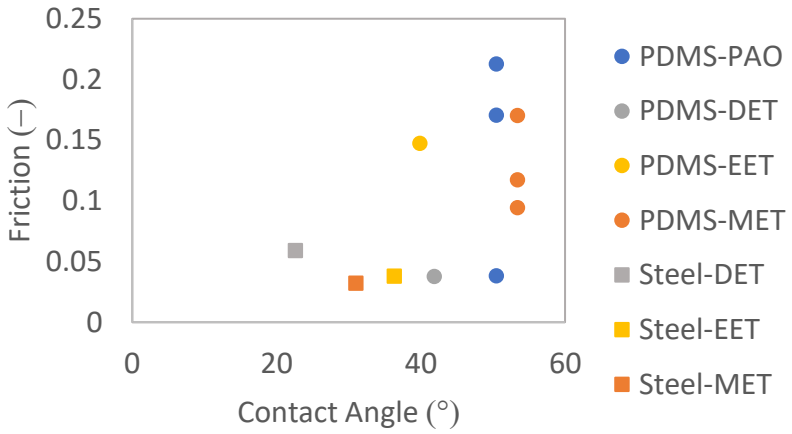

Figure 14: Average friction against contact angle for PDMS (dot) and steel (square) for PAO (blue), DET (grey), EET (yellow), and MET (orange).

Lubricant	Average Contact Angle (θ)	2*SD	SE at 2*SD
PAO40	50.44	3.62	2.09
DET	41.825	3.65	2.11
MET	53.4	0.82	0.41
EET	39.83	3.47	1.74

Table 3 Average Contact angle measurements and uncertainty based on twice of standard deviation (SD) and standard error (SE) for a confidence interval of 95% for PAO40, DET, MET, and EET on PDMS. Each measurement was taken for a time period of 300 seconds at room temperature.

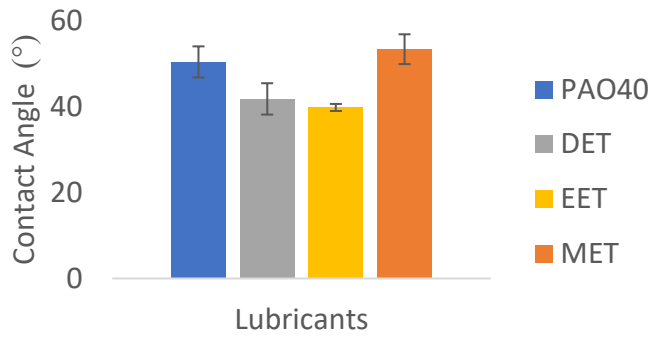

Figure 15: Average contact angle values for different lubricants on PDMS surface.

Lubricant	Average Contact Angle (θ)
DET	22.6±0.03
MET	30.96±0.01
EET	36.29±0.25

Table 4 Average contact angle measurements with uncertainty for a confidence interval of 95 % for DET, MET and EET on steel surface.

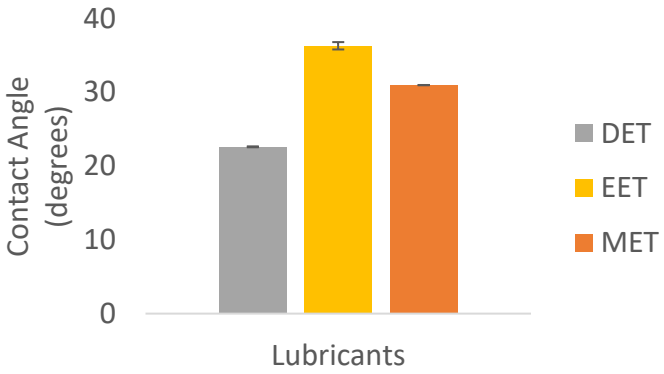

Figure 16: Average contact angle values for different lubricants on steel surface

6.3 Characterization based on non-dimensionalized spreading parameter $|S^*|$

As per Kalin et al., lower value of spreading parameter leads to lower coefficient of friction[4]. Kalin et al. made the claim for elasto-hydrodyanmic lubrication regime (EHL). The friction was expected to decrease with decrease in the value of spreading parameter if the system operates in HL regime. It was observed that for $\lambda > 3$, MET recorded a lower friction value than PAO and MET also had a lower value of S^* (Fig.25). PDMS-EET recorded an even lower value of spreading parameter but the friction values were very high. A system operating in BL was expected to experience lesser friction with increase in value of spreading parameter. PDMS-PAO system recorded a lower friction in BL than PDMS-MET in BL. The value of S^* was higher for PDMS-PAO than that for PDMS-MET. PDMS-EET recorded the highest value of S^* among all the systems that operated in HL and recorded the highest value of friction among all the HL systems studied. The value of friction was higher than anticipated. Similarly, PDMS-DET recorded the highest value of S^* and the lowest value for friction among all the PDMS systems that operated in BL, but the friction values were lower than expected. Steel-steel surfaces witnessed highest friction with DET but DET recorded the highest value of S^* on steel (Fig.17).

It was observed that any formulation of spreading parameter $(S, SP, \ or \ |S^*|)$ cannot be used alone to characterize friction when the same lubricant and surface pair is operated in different operating conditions (load and speed). The value of S^* stays constant for a system and is not affected by any change in operating conditions. In scenarios where the same system is tested under different lubrication regimes, spreading parameter alone cannot be used to characterized wettability. The friction values for PDMS-MET and PDMS-PAO pairs varied as per the operating conditions but the value of $|S^*|$ remained constant. A lot of previous studies were able to characterize friction based on spreading parameter because they operated each surface lubricant pair at one operating condition and did not alter the load and speed to obtain different operating conditions.

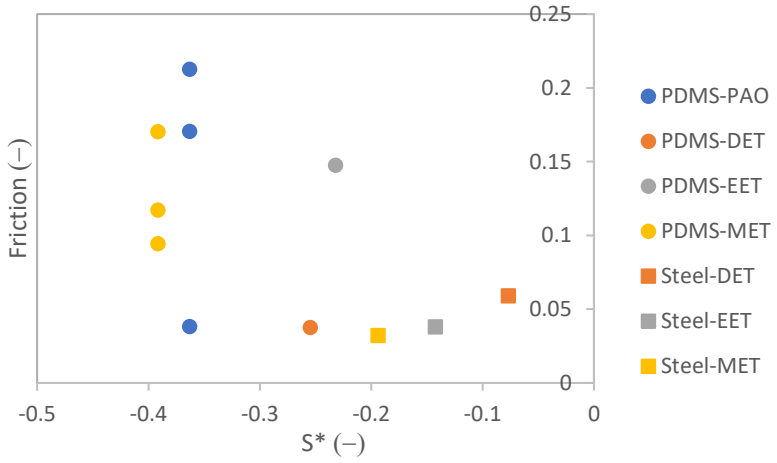

Figure 17: Friction versus S^* for PDMS-steel (dot) steel-steel (square) surface pairs for PAO (blue), DET (orange), EET (grey), and MET (yellow) at different loads and speeds.

Lubricant	$\|S^*\|$	Uncertainty
PAO40	0.3631	±0.05
DET	0.2548	±0.04
EET	0.2321	±0.04
MET	0.3917	±0.02

Table 5 Values of $|S^*|$ for different lubricants on PDMS surface with uncertainty at two standard deviations at 95 % confidence interval.

Lubricant	$\|S^*\|$	Uncertainty
DET	0.0768	±0.0002
MET	0.1425	±0.0001
EET	0.1940	±0.003

Table 6 Values of $|S^*|$ for different lubricants on steel surface with uncertainty at two standard deviations at 95 % confidence interval.

6.4 Characterization based on λ and $\lambda|S^*|$

In this study, characterization based on $\lambda|S^*|$ was different from that offered by Schertzer et al. As per Schertzer et al., a system must operate in BL if $\lambda|S^*| < 10^{-3}$, in ML if $10^{-3} < \lambda|S^*| < 0.5$, and in HL if $\lambda|S^*| > 0.5$ [6]. In this study, the friction values and λ values were compared against $\lambda|S^*|$ values. For PDMS-PAO and PDMS-MET pairs, the λ values aligned with the friction values. The values for $\lambda|S^*|$ were calculated for both the pairs (Table 2, 7, and 10). The characterization found in this study was as follows:

- A system operates in HL if $\lambda|S^*| > 1$
- A system operates in ML if $0.5 < \lambda|S^*| < 1$
- A system operates in BL if $\lambda|S^*| < 0.5$

6.4.1 PDMS and lubricants

6.4.1.1 PDMS and PAO

Based on the values of λ, the expected behavior was that friction would decrease with increase in λ. The PDMS and PAO pair was tested for a value of λ ranging from 0.86 to 3.10 (Table 7). The system would record high friction values for $\lambda < 1$ as the system operates in BL regime, moderate values for $1 < \lambda < 3$ as the system operates in ML regime, and low values for $\lambda > 3$ as the system operates in HL regime. The calculations based on $\lambda|S^*|$ characterized the lubrication like values based on λ. So, as per the friction values would also align with the characterization based on $\lambda|S^*|$. The results recorded in this

study matched all the expected results. The friction values decreased with increase in λ and aligned well with the characterization based on λ and $\lambda|S^*|$

For a λ value of 0.86 three friction tests were performed and the average value of friction for these tests was 0.22 with a standard deviation of 0.023. The friction values were high because system operated in boundary lubrication regime ($\lambda < 1$ or $\lambda|S^*| < 0.5$).

Similar behavior was observed when the PDMS and PAO pair was operated under mixed lubrication regime ($1 < \lambda < 3$ or $0.5 < \lambda|S^*| < 1$) and hydrodynamic lubrication ($\lambda > 3$ or $\lambda|S^*| > 1$) (Fig. 18). In mixed lubrication regime, the average friction value was 0.17 with a standard deviation of 0.097. In hydrodynamic lubrication regime, the average friction value was 0.098 with a standard deviation of 0.0066. Overall, the friction value was highest in boundary lubrication regime, decreased moderately in mixed lubrication regime, and was the lowest in hydrodynamic lubrication regime. Also, the characterization of friction behavior based on λ was similar to characterization based on $\lambda|S^*|$. This means that for every test case the lubrication regime pointed by value of λ and that pointed by value of $\lambda|S^*|$ were same.

λ	$\lambda\|S^*\|$	$Regime\ as\ per\ \lambda$	$Regime\ as\ per\ \lambda\|S*\|$	$\mu\ (average)$
3.095±0.003	1.124±0.2	HL	HL	0.0382±0.01
2.458±0.0003	0.892±0.1	ML	ML	0.1704±0.02
0.863±0.001	0.313±0.05	BL	BL	0.2126±0.05

Table 7 λ, $\lambda|S^*|$, lubrication regime characterization based on λ and $\lambda|S^*|$, uncertainty for λ $|S^*|$ at two standard deviations and 95 % confidence, friction results, and uncertainty in terms of twice of standard deviation (SD) and standard error (SE) at confidence interval of 95% for PAO40 and PDMS surface lubricant pair.

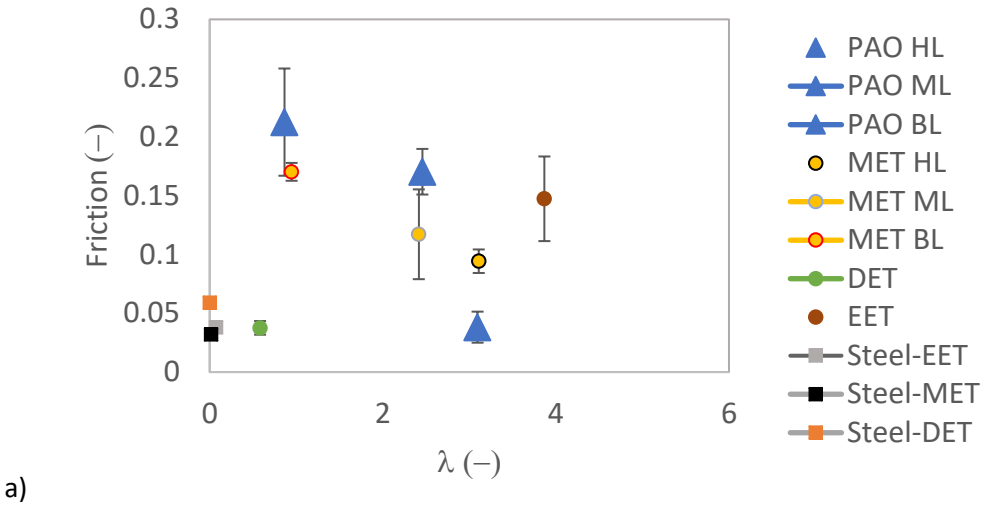

a)

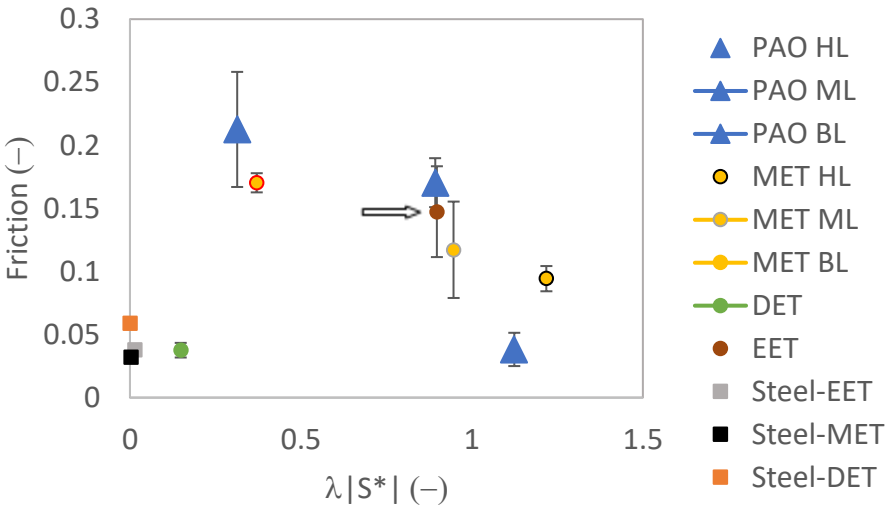

b)

Figure 18: PAO-PDMS friction values (blue triangles) against a) three values of λ: 0.86 (grey), 2.46 (orange), and 3.10 (blue) and b) three values of $\lambda|S^*|$: 0.31 (grey), 0.89 (orange), and 1.12. Characterization based on both λ and $\lambda|S^*|$ aligned with the actual results.

6.4.1.2 PDMS and Ionic Liquids

6.4.1.2.a DET

The expected behavior for DET-PDMS pair was to record high friction value. DET recorded lowest λ value (Table 8) and was the least viscous lubricant in this study. The $\lambda|S^*|$ value like λ value predicted that the system would operate in BL regime. But the actual results were different from the expectation. DET-PDMS pair recorded a very low friction value. Characterization based neither on λ nor on $\lambda|S^*|$ aligned with the friction results. The friction behavior of DET-PDMS pair was similar to a system operating in HL regime.

The average friction value was 0.0376 with a standard deviation of 0.0029. As per the friction values, the behavior of the system is similar to behavior of a system in hydrodynamic lubrication regime. A proposed reason for such a behavior is that DET when used in boundary lubrication regime reacts with steel and creates a lubrication film. This film might lower the friction. So, even when characterizations based on λ and $\lambda|S^*|$ predicted that the system would behave in boundary lubrication regime, the system recorded very low friction values. The friction values became steady from the start of the experiment (Fig. 19).

λ	$\lambda\|S^*\|$	$Regime\ as\ per\ \lambda$	$Regime\ as\ per\ \lambda\|S*\|$	$\mu\ (average)$
0.58±0.001	0.148±0.02	BL	BL	0.0376±0.006

Table 8 λ, $\lambda|S^*|$, lubrication regime characterization based on λ and $\lambda|S^*|$, uncertainty for $\lambda\ |S^*|$ at two standard deviations and 95 % confidence, friction results, and uncertainty in terms of twice of standard deviation (SD) and standard error (SE) at confidence interval of 95% for DET and PDMS surface lubricant pair.

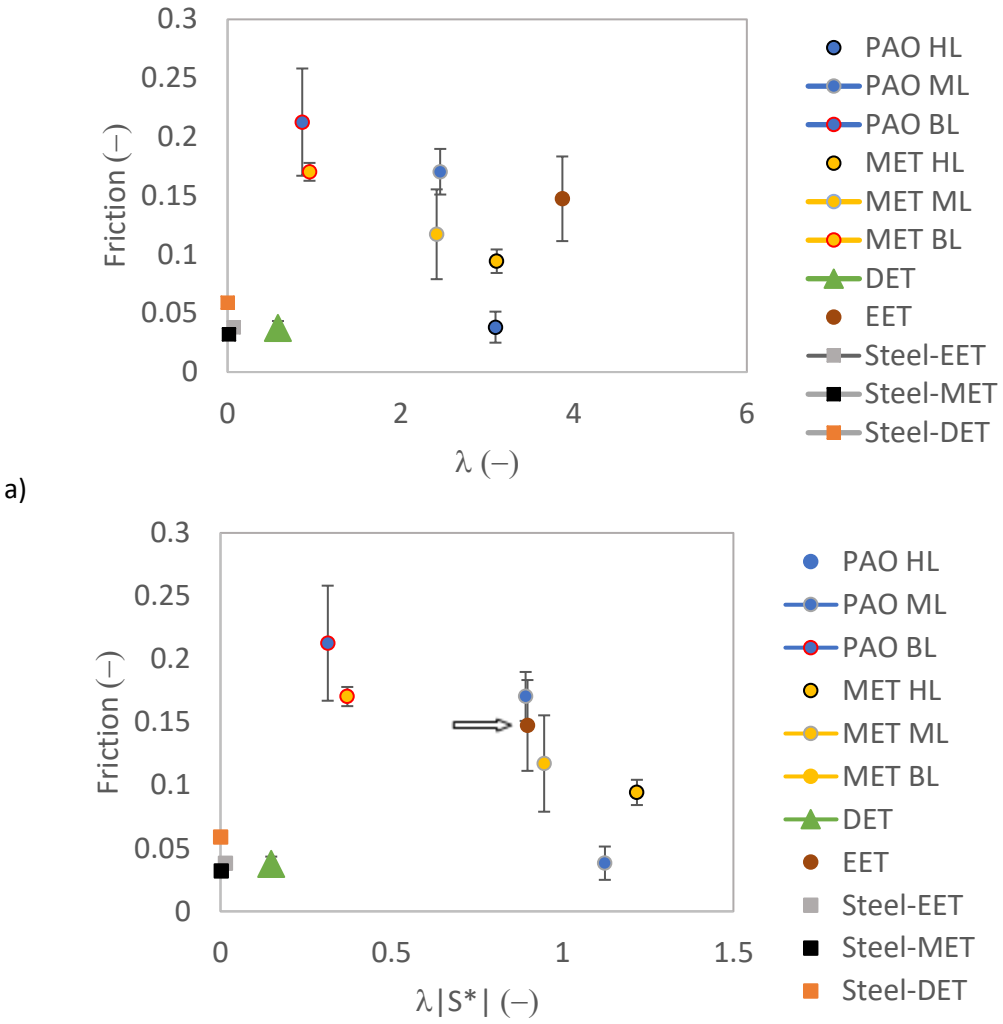

Figure 19: DET-PDMS friction value (green triangle) at a) $\lambda = 0.58$ and b) $\lambda|S^*| = 0.148$ at a sliding speed of 0.05 m/s and a load of 1 N for a sliding distance of 100 meters. Both λ and $\lambda|S^*|$ predicted the system would operate in BL ($\lambda < 1$ or $\lambda|S^*| < 0.5$). The characterization based on λ was similar to characterization based on $\lambda|S^*|$. The friction values were lower than expected and similar to that of a system in HL.

6.4.1.2.b EET

Based on the value of λ (3.86), it was expected that EET-PDMS pair would operate in HL regime and record low values of friction (Table 9). But as wetting ($|S^*|$) was included in characterization, the $\lambda|S^*|$ value (0.869) predicted that the system would operate in ML regime. Now the system was expected to align with the results based on $\lambda|S^*|$ as characterization based on λ does not take into account wettability.

The average friction value for EET and PDMS pair was 0.1338. This value is similar to the value obtained for a system operating in mixed lubrication regime. Hence, the characterization based on $\lambda|S^*|$ better predicted the friction behavior of the system that the characterization based on λ (Fig. 20).

λ	$\lambda\|S^*\|$	$Regime\ as\ per\ \lambda$	$Regime\ as\ per\ \lambda\|S*\|$	$\mu\ (average)$
3.86±0.001	0.869±0.1	HL	ML	0.1474±0.036

Table 9 λ, $\lambda|S^*|$, lubrication regime characterization based on λ and $\lambda|S^*|$, friction results, and uncertainty in terms of twice of standard deviation (SD) and standard error (SE) at confidence interval of 95% for EET and PDMS surface lubricant pair.

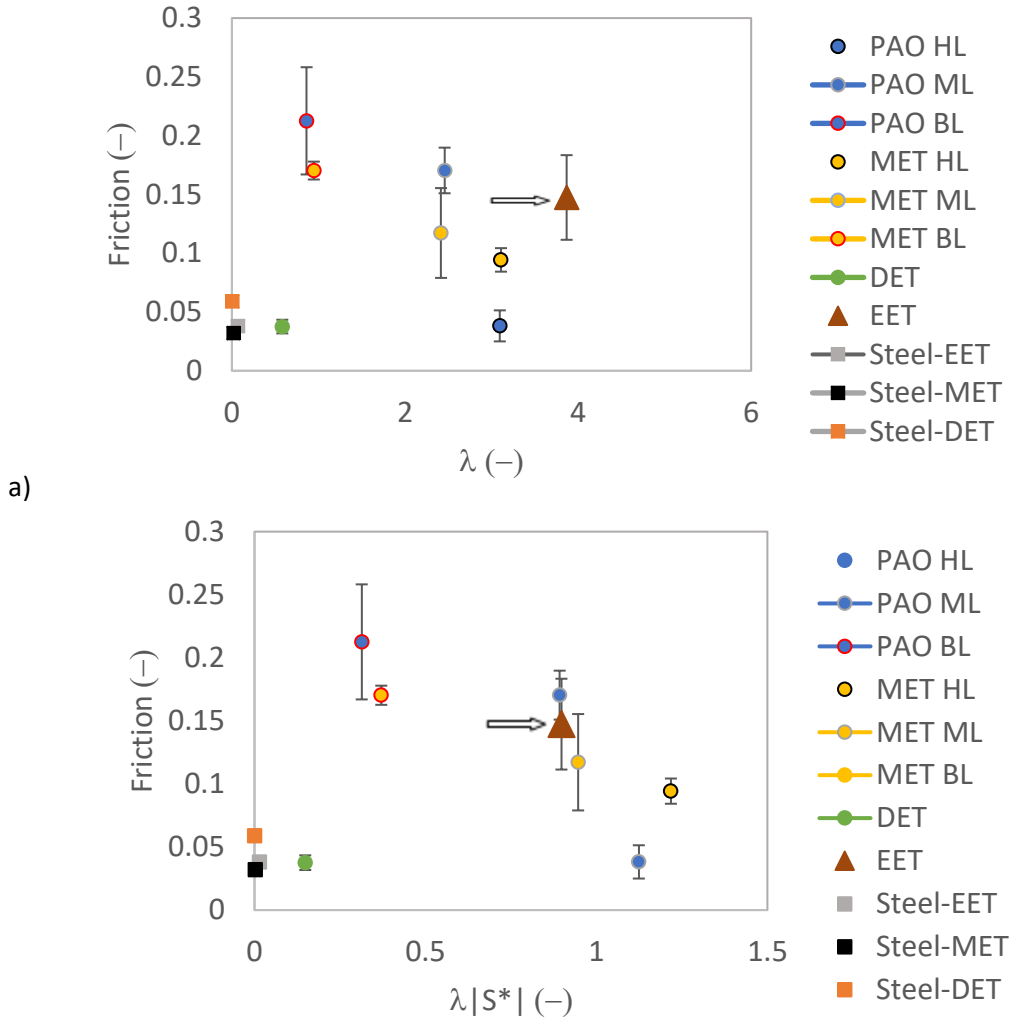

Figure 20: EET-PDMS friction value (red triangle) at a) $\lambda = 3.86$ and b) $\lambda|S^*| = 0.869$ at speed of 0.01 m/s and applied load of 3.98 N for a sliding distance of 100 meters. The λ value predicted the system would operate in HL $(\lambda > 3)$ but the $\lambda|S^*|$ predicted the system would operate in ML $(0.5 < \lambda|S^*| < 1)$. The characterization based on $\lambda|S^*|$ better aligned with the actual results.

6.4.1.2.c MET

Based on values of λ, it was expected that MET-PDMS pair would operate in all three regimes and that friction value will decrease as the lubrication regime moves from BL to HL regime. For PDMS-MET pair, the surface lubricant pair was tested for λ ranging from 0.946 to 3.109 (Table 10). The characterizations based on λ and $\lambda|S^*|$ were similar.

The friction results were expected to align with both the characterizations. In BL regime ($\lambda < 1 \ or \ \lambda|S^*| < 0.5$) the average friction value after 4 tests was 0.1703 with a standard deviation of 0.0038.

In ML regime ($1 < \lambda < 3 \ or \ 0.5 < \lambda|S^*| < 1$), the average friction value was 0.1172 with a standard deviation of 0.0191. In HL regime ($\lambda > 3 \ or \ \lambda|S^*| > 1$), the average friction value was 0.0943. Lowest friction values were recorded for HL regime and friction value increased as we moved from HL to BL regime. The friction results aligned with characterization based on λ and that based on $\lambda|S^*|$ (Fig 21).

λ	$\lambda\|S^*\|$	$Regime\ as\ per\ \lambda$	$Regime\ as\ per\ \lambda\|S*\|$	$\mu\ (average)$
3.109±0.003	1.218±0.06	HL	HL	0.0943±0.01
2.416±0.003	0.946±0.05	ML	ML	0.1172±0.04
0.889±0.007	0.348±0.02	BL	BL	0.1703±0.003

Table 10 λ, $\lambda|S^*|$, lubrication regime characterization based on λ and $\lambda|S^*|$, uncertainty for $\lambda\ |S^*|$ at two standard deviations and 95 % confidence, friction results, and uncertainty in terms of twice of standard deviation (SD) and standard error (SE) at confidence interval of 95% for MET and PDMS surface lubricant pair.

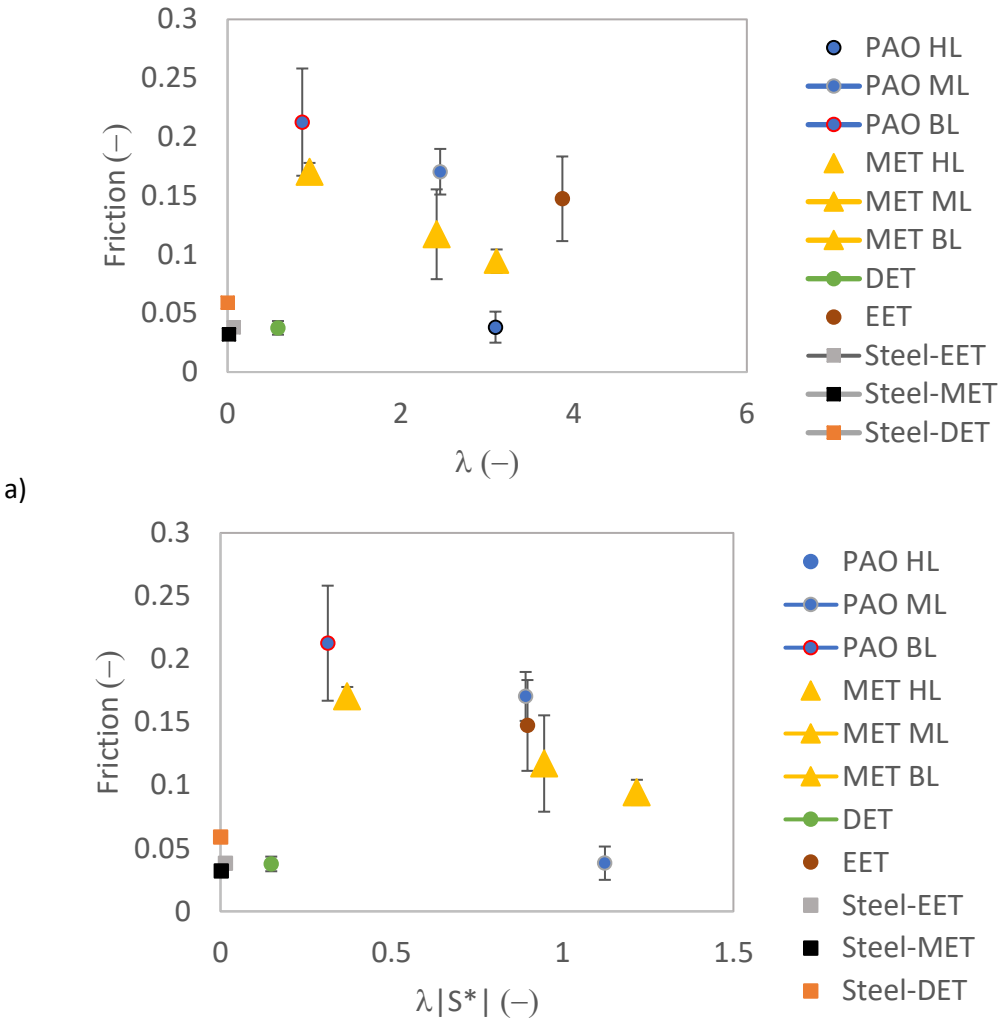

Figure 21: MET-PDMS friction values (yellow triangles) against a) three values of λ: 0.946 (grey), 2.416 (orange), and 3.109 (blue) and b) three values of $\lambda|S^*|$: 0.371 (grey), 0.946 (orange), and 1.218.

6.5 Steel and Ionic Liquids

The data for steel-steel surface pair and ionic liquids as lubricant was collected by Hong Guo (Table 11).

Lubricant	λ	$\lambda\|S^*\|$	$Regime\ as\ per\ \lambda$	$Regime\ as\ per\ \lambda\|S*\|$	$\mu\ (average)$
DET	0.00291± 0.0003	0.0022± 0.00002	BL	BL	0.059± 0.0004
EET	0.07361± 0.008	0.0143± 0.02	BL	BL	0.038± 0.001
MET	0.01694± 0.002	0.0024± 0.0003	BL	BL	0.032± 0.001

Table 11 λ, $\lambda|S^*|$, lubrication regime characterization based on λ and $\lambda|S^*|$, uncertainty for $\lambda\ |S^*|$ at two standard deviations and 95 % confidence, friction results, and uncertainty in terms of twice of standard deviation (SD) and standard error (SE) at confidence interval of 95% for different lubricants on steel.

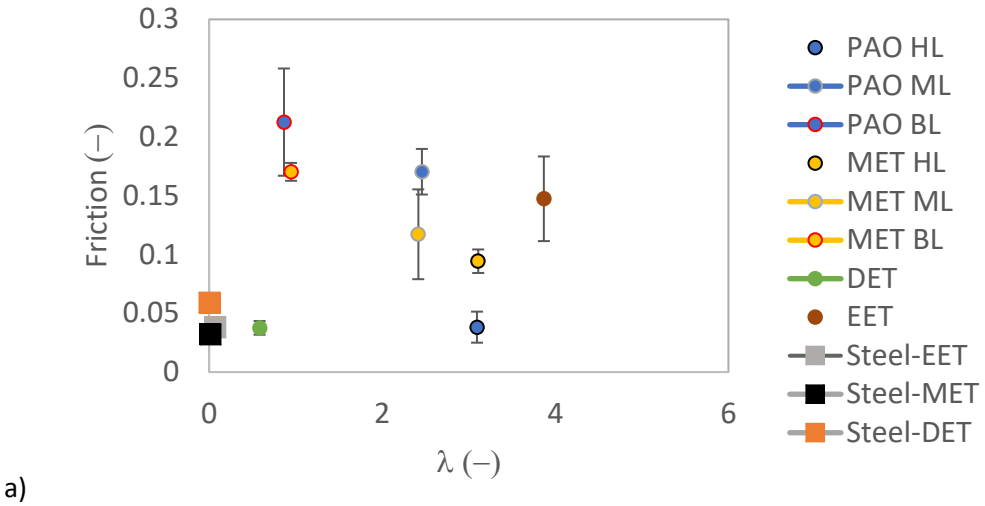

a)

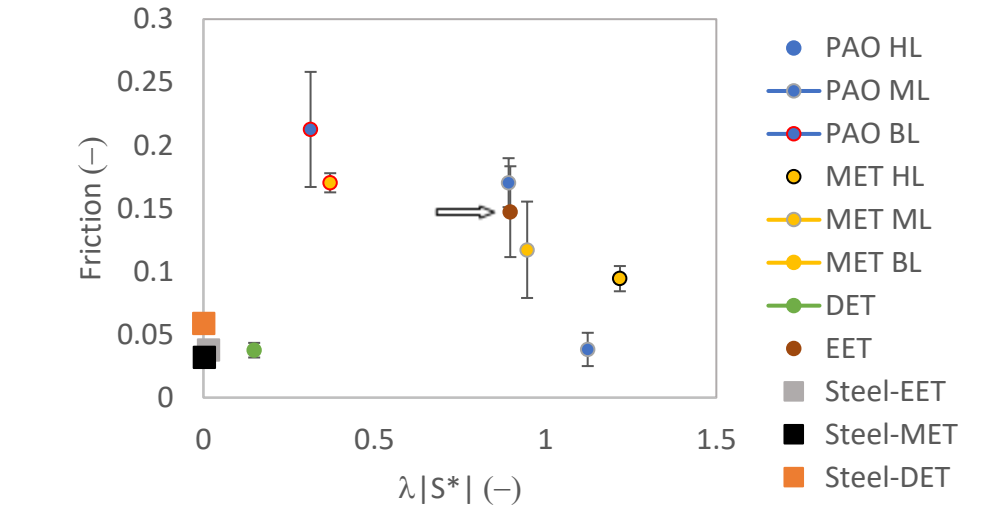

b)

Figure 22: Friction values (squares) for different lubricants on steel surface against a) λ: 0.003 for DET (blue), 0.074 for EET (grey), and 0.017 for MET (orange), and b) $\lambda|S^*|$: 0.0002 for DET (blue), 0.0142 for EET (grey), and 0.0024 for MET (orange).

Based on values of λ, the three lubricants were expected to operate in BL regime with steel. The lambda (λ) values for all three lubricants when used with steel as surface were less than one. The characterization based on $\lambda|S^*|$ was similar to that based on λ (Table 11). The systems were expected to record high friction values. But the friction values for all the lubricants were very low. The friction behavior of each lubricant with steel was similar to that of a system operating in HL regime.

Steel-DET pair recorded an average friction of 0.059 with a standard deviation of 0.000212. DET recorded the highest friction with steel in comparison to other lubricants. MET with steel recorded an average friction of 0.032 with a standard deviation of 0.000707. This was the lowest value for friction for any lubricant with steel. EET recorded an average friction of 0.038 with a standard

deviation of 0.000495 (Fig. 22). But in all the cases, the friction was much lower than anticipated friction values. A plausible explanation for such a behavior would be that the three ionic liquids undergo a chemical reaction with the steel surface, forming a fluid film. This fluid film might then result in lower friction values.

6.6 Summary

It was expected that different data points for different surface-lubricant pairs operated under different operating conditions would collapse into one friction versus $\lambda|S^*|$ curve. In this study, characterization based on $\lambda|S^*|$ witnessed some outliers. PDMS-DET pair and all the cases involving steel did not output friction as expected. The friction values were very low and were similar to values observed in any system operating in HL, but the value of $\lambda|S^*|$ for each of these systems predicted that the system would operate in BL. For all other cases, the characterization based on $\lambda|S^*|$ aligned with the actual results. It was observed that different data points, except outliers, did align together (Fig.23)).

In one case the characterization based on $\lambda|S^*|$ was better that that based on λ. In case of PDMS-EET pair, the λ value (3.86) predicted that the system would operate in HL but the $\lambda|S^*|$ value (0.86) predicted that the system would operate in ML. The actual performance of the system aligned with the value based on $\lambda|S^*|$. The high value of λ was adjusted by small value ofS^* to give a moderate value of friction. This observation suggests that neither λ nor S^* (spreading parameter) should be used alone to characterize friction, rather a combination of both ($\lambda|S^*|$) should be used.

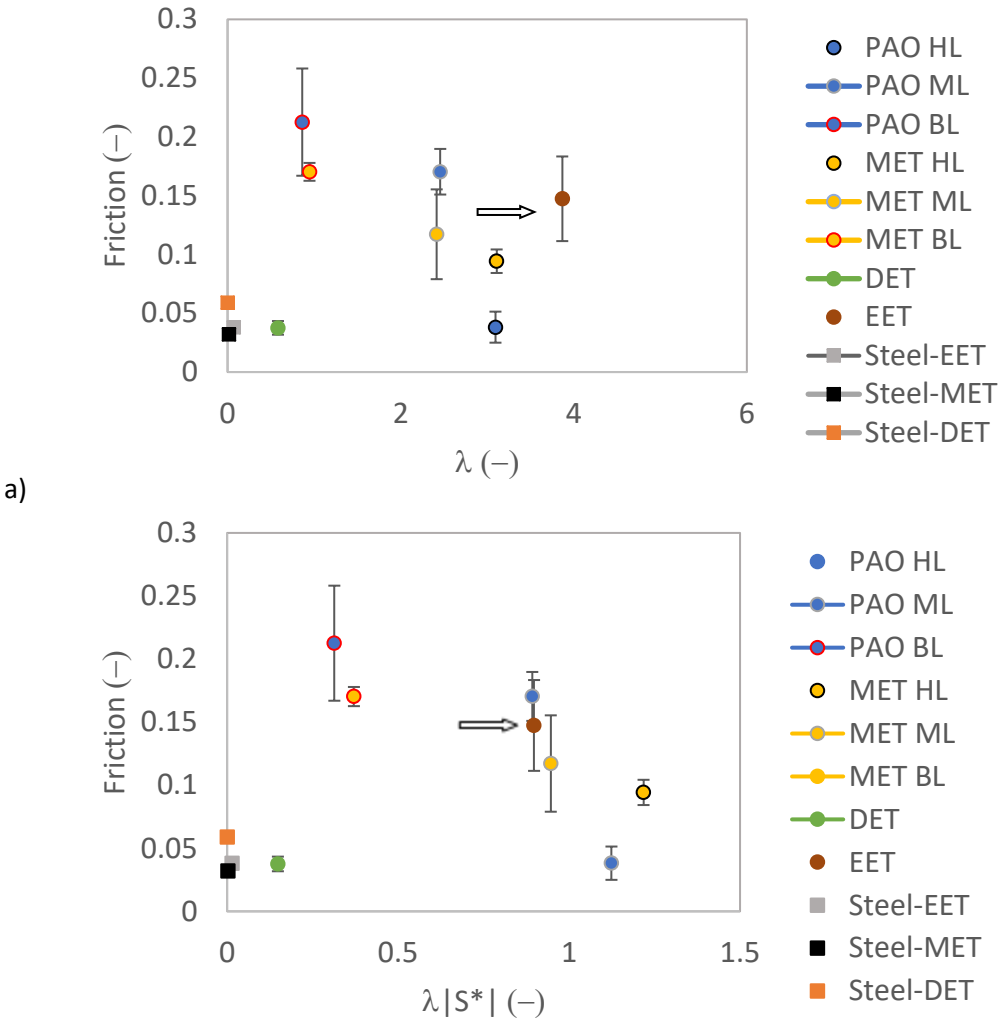

a)

b)

Figure 23: Combined friction values for steel and PDMS surfaces and DET, EET, and MET lubricants against a) λ and b) $\lambda|S^*|$. The arrows point out that PDMS-EET test case operated in ML regime as predicted by value of $\lambda|S^*|$ and not in HL regime as predicted by value of λ. The arrow indicates the PDMS-EET case in which λ predicted HL regime anf $\lambda|S^*|$ predicted ML regime. This case operated in ML.

7.0 Conclusion

- Contact angle measurements cannot be used to characterize friction when a surface lubricant pair is operated under different operating conditions. For a surface lubricant pair, the friction behavior changed with operating conditions.
- For most of the test cases, the characterization based on λ was similar to characterization based on $\lambda|S^*|$. But in one test case of PDMS-EET pair the λ value predicted that the system would operate in HL regime and $\lambda|S^*|$ value predicted that the system would operate in ML regime. Based on the friction values it was found that prediction based on $\lambda|S^*|$ was more accurate.
- There were some outliers in the study. DET-PDMS pair recorded very low friction values but the λ and $\lambda|S^*|$ values predicted that the system would operate in boundary lubrication regime. Also, when steel was used as the surface, all the lubricants recorded very low friction values but λ and $\lambda|S^*|$ values predicted that the system would operate in boundary lubrication regime. One plausible explanation for this deviant behavior would be that all the ionic liquids react with the steel surface and form a lubricant film. This film then helps in reducing friction.

8.0 Future Work

- The effect of change in surface roughness of soft surface in case of soft surface and hard surface pair should be taken into consideration. The change in surface roughness might alter surface properties (specific film thickness). This change in surface properties might alter friction behavior.
- A study should be conducted to analyze tribological behavior of a system that uses same polymer for both the surfaces. This study will help avoid the possibility of any chemical reaction between lubricant and any of the surfaces.
- Analysis should be conducted for metal-metal surface pairs in which different lubrication regimes can be reached. Such an analysis will help analyze and characterize wear behavior. This study will also help characterize friction for hard-hard surface pair.
- This study was not able to characterize friction for some outliers. A possible explanation for such a behavior might be that lubricant reacted with the surface and formed a fluid film. This fluid film might have then altered some surface properties and reduced friction. Future studies should analyze wetting behavior before and after the experiments to look for any change. If the wettability of the system changes after the reaction then this change might explain the different behavior observed in the outliers.

9.0 Bibliography

[1] Lev, A., 1999, “Energy Efficiency of Industrial Oils.”

[2] Bombard, A. J. F., and Vicente, J. De, 2012, “Boundary Lubrication of Magnetorheological Fluids in PTFE / Steel Point Contacts,” Wear, **296**(1–2), pp. 484–490.

[3] Kalin, M., and Polajnar, M., 2014, “The Wetting of Steel, DLC Coatings, Ceramics and Polymers with Oils and Water: The Importance and Correlations of Surface Energy, Surface Tension, Contact Angle and Spreading,” Appl. Surf. Sci., **293**, pp. 97–108.

[4] Kalin, M., and Polajnar, M., 2013, “The Effect of Wetting and Surface Energy on the Friction and Slip in Oil-Lubricated Contacts,” Tribol. Lett., **52**(2), pp. 185–194.

[5] Kalin, M., and Polajnar, M., 2013, “The Correlation between the Surface Energy, the Contact Angle and the Spreading Parameter, and Their Relevance for the Wetting Behaviour of DLC with Lubricating Oils,” Tribol. Int., **66**, pp. 225–233.

[6] Schertzer, M., and Iglesias, P., 2018, “Meta-Analysis Comparing Wettability Parameters and the Effect of Wettability on Friction Coefficient in Lubrication,” Lubricants, **6**(3), p. 70.

[7] Velkavrh, I., and Kalin, M., 2012, “Tribology International Comparison of the Effects of the Lubricant-Molecule Chain Length and the Viscosity on the Friction and Wear of Diamond-like-Carbon Coatings and Steel,” Tribiology Int., **50**, pp. 57–65.

[8] Kalin, M., Velkavrh, I., and Viˇ, J., 2009, “The Stribeck Curve and Lubrication Design for Non-Fully Wetted Surfaces,” **267**, pp. 1232–1240.

[9] Bombard, A. J. F., Gonçalves, F. R., Shahrivar, K., Ortiz, A. L., and de Vicente, J., 2015, “Tribological Behavior of Ionic Liquid-Based Magnetorheological Fluids in Steel and Polymeric Point Contacts,” Tribol. Int., **81**, pp. 309–320.

[10] Bombard, A. J. F., Vicente, J. De, and Rheology, W. Á. I. Á., 2012, “Thin-Film Rheology and Tribology of Magnetorheological Fluids in Isoviscous-EHL Contacts,” pp. 149–162.

[11] Bombard, A. J. F., Gonc¸alves, F. R., Shahrivar, K., Ortiz, A. L., and De Vicente, J., 2014, “Tribological Behavior of Ionic Liquid-Based Magnetorheological Fluids in Steel and Polymeric Point Contacts,” Tribol. Int., **81**, pp. 309–320.

[12] Bhushan, B., 2013, “No Title,” Introd. to Tribol., **2nd Editio**.

[13] Tzanakis, I., Hadfield, M., Thomas, B., Noya, S. M., Henshaw, I., and Austen, S., 2012, “Future Perspectives on Sustainable Tribology,” Renew. Sustain. Energy Rev., **16**(6), pp. 4126–4140.

[14] Craig, V. S. J., Neto, C., and Williams, D. R. M., 2001, “Shear-Dependent Boundary Slip in an Aqueous Newtonian Liquid,” pp. 1–4.

[15] Lubrecht, A. A., Venner, C. H., and Colin, F., 2009, “Film Thickness Calculation in Elasto-Hydrodynamic Lubricated Line and Elliptical Contacts: The Dowson, Higginson, Hamrock Contribution,” Proc. Inst. Mech. Eng. Part J J. Eng. Tribol., **223**(3), pp. 511–515.

[16] “Dowson Original.Pdf.”

[17] Dowson, D., and Bernard, J., 1977, “Elastohydrodynamic Lubrication of Elliptical Contracts for Materials of Low Elastic Modulus : I . Fully Flooded Conjunction / Bernard J . Public Domain , Google-Digitized,” **100**(April).

[18] Hamrock, B. J., and Dowson, D., 1977, “Isothermal Elastohydrodynamic Lubrication of Point Contacts: Part III—Fully Flooded Results,” J. Lubr. Technol., **99**(2), p. 264.

[19] Persson, B. N. ., 2000, *Sliding Friction: Physical Principles and Applications*, Berlin; New York: Springer, 2000.

[20] Smeeth, M., and Spikes, H. A., 1997, “Central and Minimum Elastohydrodynamic Film Thickness at High Contact Pressure,” J. Tribol., **119**(2), pp. 291–296.

[21] Janardhanan, K., and Iglesias, P., 2016, “Theoretical and Experimental Study of the Friction Behavior of Halogen-Free Ionic Liquids in Elastohydrodynamic Regime,” Lubricants, **4**(2), p. 16.

[22] Hamrock, B. J., and Dowson, D., 1977, “Isothermal Elastohydrodynamic Lubrication of Point Contacts Part III — Fully Flooded Results,” (April), pp. 264–275.

[23] Van Leeuwen, H., 2011, “The Determination of the Pressure-Viscosity Coefficient of a Lubricant through an Accurate Film Thickness Formula and Accurate Film Thickness Measurements. Part 2: High L Values,” Proc. Inst. Mech. Eng. Part J J. Eng. Tribol., **225**(6), pp. 449–464.

[24] Verkrijging, T. E. R., Doctor, V. A. N. D. E. G. V. A. N., Wetenschappen, T., Technische, A. A. N. D. E., Delft, H. T. E., Rector, O. P. G. V. A. N. D. E., Mijnbouwkunde, D. E. L. D. E. R., and Commissie, V. E. E. N., 1966, “Correlational Aspects of the Viscosity · Temperature · Pressure Relationship,” (April).

[25] Fowkes, F. M., “Attractive Forces at Interfaces.”

[26] Owens DK, W., 1969, “Estimation of the Surface Free Energy of Polymers.,” J. Appl. Polym. Sci.

[27] CM., M., *Tribology on the Small Scale*.

[28] Matczak, L., Johanning, C., Gil, E., Guo, H., Smith, T. W., Schertzer, M., and Iglesias, P., 2018, “Effect of Cation Nature on the Lubricating and Physicochemical Properties of Three Ionic Liquids,” Tribol. Int., **124**(December 2017), pp. 23–33.

[29] Guo, H., Smith, T. W., and Iglesias, P., 2019, “The Study of Hexanoate-Based Protic Ionic Liquids Used as Lubricants in Steel-Steel Contact,” J. Mol. Liq., (xxxx), p. 112208.

[30] Thomas Zolper, 2012, “Lubrication Properties of Polyalphaolefin and Polysiloxane Lubricants: Molecular Structure–Tribology Relationships,” Tribol. Lett.

[31] Sameer, “Ball on Flat Tribometer Procedure.”

[32] Charu Dwivedi, S. P., 2017, “Electrospun Nanofibrous Scaffold as a Potential Carrier of Antimicrobial Therapeutics for Diabetic Wound Healing and Tissue Regeneration,” *Nano- and Microscale Drug Delivery Systems*.